Summer 8-2018

# Characterizing the Role for the Timeless Gene in Planarian Regeneration

Suzanne Craig

# CHARACTERIZING THE ROLE FOR THE *TIMELESS* GENE IN PLANARIAN REGENERATION

A Thesis

Submitted to the School of Graduate Studies and Research

in Partial Fulfillment of the

Requirements for the Degree

Master of Science

Suzanne Elizabeth Craig

Indiana University of Pennsylvania

August 2018

Indiana University of Pennsylvania
School of Graduate Studies and Research
Department of Biology

We hereby approve the thesis of

Suzanne Elizabeth Craig

Candidate for the degree of Master of Science

_____ _____
Robert Major, Ph.D.
Associate Professor of Biology, Advisor

_____ _____
Robert Hinrichsen, Ph.D.
Professor of Biology

_____ _____
Christine Ruby, Ph.D.
Assistant Professor of Biology

ACCEPTED

_____ _____
Randy L. Martin, Ph.D.
Dean
School of Graduate Studies and Research

Title: Characterizing the Role for the *Timeless* Gene in Planarian Regeneration

Author: Suzanne Elizabeth Craig

Thesis Chair: Dr. Robert Major

Thesis Committee Members: Dr. Robert Hinrichsen
Dr. Christina Ruby

The regeneration capabilities of humans are limited. In contrast, planarians have incredible regeneration capabilities. Recently, planarians have become a popular model system for studying regeneration mechanisms. The remarkable regeneration abilities of planarians are derived from a population of adult stem cells called neoblasts. Previous results from our laboratory revealed that a circadian rhythm gene, called *timeless*, produces phenotypes associated with neoblast deficiency. The circadian clock has relationships with both the cell cycle and stem cell control, but the role of circadian rhythms and clock genes in regeneration is not understood. We found that targeting *timeless* for dsRNA interference significantly reduced the amount of mitotic neoblasts in both whole planarians and amputated fragments. This demonstrates a role for timeless in the control of neoblast proliferation. We hypothesize that *timeless* is a communication link between circadian rhythms and cell cycle control and uses these pathways to control neoblast function during regeneration.

ACKNOWLEDGEMENTS

I would like to thank Dr. Major for accepting me into his lab as a returning student to the scientific world. I am so thankful that I was welcomed into a lab that felt like a family and had the chance to pursue a degree that I am so passionate about. I appreciate the time, discussions, guidance and emotional support that Dr. Major provided to me any time I needed it. I became the scientist I am today through this mentorship. I would like to thank my committee, Dr. Hinrichsen and Dr. Ruby, for their enthusiasm and guidance. I would like to also thank Dr. Hinrichsen for the many hours of coursework that I learned in class and the freedom to pursue topics of interest for my term papers. I will always keep the spirit of curiosity that I learned through these projects.

Lastly, I would like to thank my friends and family for their unconditional support through this process, and for so strongly affirming that I was meant for this path. I could never have come this far without your love and support. Thank you and I love you all so much.

TABLE OF CONTENTS

LIST OF FIGURES

# CHAPTER 1

## INTRODUCTION

Humans cannot regenerate vital tissues such as the heart or central nervous system. Damage to these tissues results in incomplete healing or the formation of scar tissue (Nakada, Levi, & Morrison, 2011; Poss, 2002). Organisms need the ability to control proliferation as a means of survival (Pearson & Sánchez Alvarado, 2009). Stem cells exist in adult tissues such as the brain, blood and gut, to replenish cellular populations that diminish through: "turnover, injury, and disease." The defining characteristic of stem cells is their ability to "remain undifferentiated". Stem cells are acted upon by a plethora of regulators that instruct their function and allow them to adapt to various physiological conditions. As organisms age, the effectiveness of stem cells begins to decline and the ability to regenerate tissues properly is diminished. One of the factors associated with this diminished ability is the agglomeration of DNA damage (Nakada et al., 2011). In the same token, inappropriate stem cell divisions and activities lead to higher incidence of cancer (Bell & Van Zant, 2004; Nakada et al., 2011). DNA damage and decreases in damage repair proteins impair stem cell functions, reduce stem cell ability to perform under biological stress, and cause "phenotypes that resemble premature aging" (Nakada et al., 2011). Stem cells are responsible for much of the regeneration processes that occur in the adult, such as responding to injury, but their incorporation into new tissues is often flawed or incomplete, leading to incomplete healing. A prime example of this is brain cells that are lost during a stroke. While neural stem cells do recover lost tissue, new neurons produced during this process do not merge with existing neural processes and therefore do not contribute to any circuitry recovery. Although this type of healing is impaired, it reveals that regeneration

systems do exist in the human (Nakada et al., 2011). Understanding the mechanisms behind regeneration may lead to pathway targets for therapeutics.

Planarians are an essential model system for studying the mechanisms of tissue regeneration. They are a small, freshwater flatworm with the amazing capability of regenerating all of their bodily systems from even tiny fragments. (Liu et al., 2013; Rink, 2013). Planarians accomplish this remarkable task through a population of stem cells, referred to as neoblasts. Neoblasts migrate to the site of injury and begin to proliferate, forming a structure of new cells called a blastema. New tissues arise as a result of this blastema formation (Elliott & Sánchez Alvarado, 2013; Reddien & Alvarado, 2004; Rink, 2013). The mechanistic pathways behind the workings of neoblasts are still not well understood, and their study presents an interesting venture into regenerative biology (Rink, 2013). Advancements in multiple cell biology techniques have opened many avenues for studying these mechanisms (Forsthoefel, Waters, & Newmark, 2014; King & Newmark, 2013; Newmark & Sánchez Alvarado, 2000; Sanchez Alvarado & Newmark, 1999).

Previous work in Dr. Major's laboratory revealed that using double-stranded RNA interference to target a particular gene in the planarian, called *timeless*, resulted in the loss of blastema formation during the regenerative process (Figure 1). Canonically, timeless is a circadian rhythm gene. However, additional pathways involving *timeless*, and a similar gene, *timeout*, are beginning to highlight a larger role for traditionally described circadian genes (Chou & Elledge, 2006; Gotter, Suppa, & Emanuel, 2008; Mazzoccoli, Laukkanen, Vinciguerra, Colangelo, & Colantuoni, 2016). Timeless may represent a link between circadian rhythms and cell cycle control (Ünsal-Kaçmaz, Mullen, Kaufmann, & Sancar, 2005). The cell cycle and circadian rhythm are very similar oscillation-based systems, but their exact relationship is not

well understood (Hunt & Sassone-Corsi, 2007). We expect that the cell cycle would be important during regeneration, after all, proliferation is one of the key components of regeneration as it requires de novo tissue generation (Elliott & Sánchez Alvarado, 2013). Less expected is that circadian rhythm genes may also be involved in an appropriate regeneration response.

Recently, the importance of cellular timing to human medicine is catching on and has led to the burgeoning field of chronotherapy, which focuses on the timing of therapeutic application (Ünsal-Kaçmaz et al., 2005). For example, it has been shown that circadian rhythms effect the success of bone marrow transplants and chemotherapeutic tactics (Nakada et al., 2011). In the fields of regeneration, circadian rhythms have been shown to contribute to the stem cell activities of the hematopoietic system (Nakada et al., 2011). Markedly, aberrant expression of *Timeless* has been shown in breast tumors (Mazzoccoli et al., 2016). Timeless presents a unique opportunity to study the mechanistic processes of tissue regeneration while also observing the effects of circadian rhythms on regeneration and the cell cycle and may provide insight into the cryptic characterization of circadian rhythm genes. My thesis project seeks to characterize the role for the circadian gene timeless in planarian regeneration.

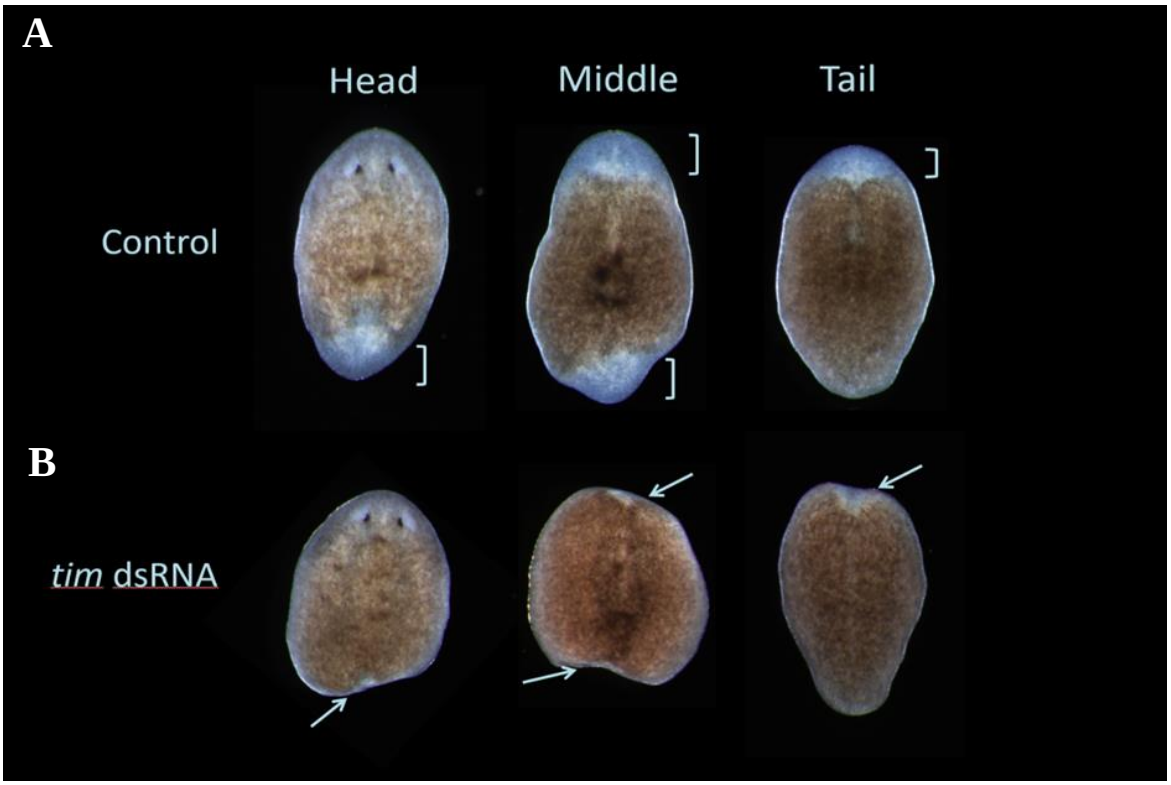


*Figure 1*. Loss of blastema formation in dsRNA treated planarians. A). Normal blastema formation (white brackets) across three amputation sites (head, middle, tail) in the control group planarians. B). Using dsRNA interference to target the function of timeless results in a lack of blastema formation (white arrows) across all amputation sites.

# CHAPTER 2

# LITERATURE REVIEW

## Planarian: *Schmidtea mediterranea*

Interest in the phenomenon of tissue regeneration has long held planarians in the eye of scientists throughout the centuries. Studies of planarian regeneration began during the late 19th century and early 20th century, when experimental embryology gained momentum, sparked by the investigation of regeneration in other organisms. The first recorded observation of regeneration came from Aristotle's observation of lizard tail regeneration around 350 BCE (Elliott & Sánchez Alvarado, 2013). Initial observations of planarian regeneration can be dated back to Pallas in 1774 (Elliott & Sánchez Alvarado, 2013; Reddien & Alvarado, 2004). During their discoveries in the 19th century, scientists remarked on the notorious regeneration abilities of planarians by describing them as "immortal under the edge of the knife" (Elliott & Sánchez Alvarado, 2013). Truly, the regeneration abilities of the planarian are remarkable. Planarians can successfully maintain their tissues through regeneration for decades, with no decline in ability. Even more, planarians seem to be outside the reach of ageing at all (Elliott & Sánchez Alvarado, 2013; Rink, 2013). Rink captured the essence of their ability with the phrase, "akin to mythological beasts, they have the ability to regenerate in their entirety even from tiny injury remnants and the asexual strains appear to be exempt from the mortal's plight of physiological ageing" (Rink, 2013).

Despite the obvious advantageousness of being able to regenerate, there's a certain unpredictability to regeneration abilities. Even amongst planarian species, regenerative ability is not universal. While regenerative ability is common for *Schmidtea mediterranea* and *Dugesia japonica, D. laceteum* is not able to regenerate in the same way. *D. lacetum* is not able to

regenerate posterior fragments, due to upregulated *Wnt* signaling. However, using RNAi for Dlac-beta-Catenin-1, researchers were able to restore posterior regeneration. Lack of regeneration between *S.meds, D.japs,* and *D.lac* show how unpredictable regenerative ability is, but also offers positive outlook for the rescue of regeneration through mechanistic understanding (Liu et al., 2013).

The planarian species *S. mediterranea* makes an excellent model for studying the mechanisms of tissue regeneration. In addition to their stated regenerative abilities, these planarians possess important qualities that make them suitable for inquiries involving human disease. They are triploblastic and have tissue types in accordance to all three germ layers: ectoderm, mesoderm and endoderm. Despite having a simple body plan, planarians possess important, recognizable organ systems that correspond to human anatomy, such as the nervous system (Elliott & Sánchez Alvarado, 2013; Rink, 2013). Additionally, there is now a complete genome and updated, efficient RNAi screening techniques (Danielle Wenemoser; Peter W. Reddien, 2011). As this species is the primary species of study in further discussions regarding regeneration, the term 'planarian' will be used in reference to *S. mediterranea.*

## Planarian Regeneration

The regeneration feats of planarians are remarkable (Liu et al., 2013; Reddien & Alvarado, 2004). Regeneration is most simply defined by Reddien and Alvarado as "the replacement of missing structures following injury" (Reddien & Alvarado, 2004). However, there are far more complicated cellular and molecular forces at work, leading to the complexity of the regeneration system (Danielle Wenemoser; Peter W. Reddien, 2011). For simplicity, regeneration can be divided into two processes: proliferation and morphallaxis (Reddien & Alvarado, 2004). Planarian regeneration is 'epimorphosis', or de novo tissue generation. This,

coupled with ‘morphallaxis,’ or reorganization of existing tissues, contributes to regeneration (Elliott & Sánchez Alvarado, 2013). In this review, emphasis will be placed on the process of epimorphosis. Injury to the planarian results in restorative regeneration, and is the sole effector of this process (Elliott & Sánchez Alvarado, 2013; Reddien & Alvarado, 2004). The process of regeneration begins with a muscular contraction at the site of amputation which minimizes the surface area of the wound. It is then covered by a thin epithelial layer that is created by cells spreading across the surface, in the absence of proliferation. Following wound closure, regenerative proliferation, or epimorphosis, is marked by a burst of cell division six hours after initial wounding. The following events of regeneration occur over the course of the next 1-2 weeks (Elliott & Sánchez Alvarado, 2013; Reddien & Alvarado, 2004; Rink, 2013). The regeneration process results in an increase in proliferating cells, which contribute to an unpigmented mass known as a blastema (Elliott & Sánchez Alvarado, 2013; Reddien & Alvarado, 2004). New tissues for the regenerating planarian are derived from this blastema (Elliott & Sánchez Alvarado, 2013).

## Neoblasts

The key to planarian regeneration lies within a population of stem cells in the planarian, called neoblasts. Neoblasts are a small population of adult parenchymal cells between 6 and 12 micrometers in diameter, that have large nuclei and very little cytoplasm. Neoblasts have a vital role to the health and maintenance of the planarian; these cells undergo proliferation to contribute to continuous cell turnover in the planarian and are responsible for producing new tissue in the form of the blastema (Elliott & Sánchez Alvarado, 2013; Reddien & Alvarado, 2004; Rink, 2013; Sánchez Alvarado, 2006). furthermore, neoblasts are the only dividing cells in the planarian (Reddien & Alvarado, 2004). Because cell divisions only occur within the neoblast

population, markers of cell division such as phospho-histone H3 are indicative of mitotic neoblasts (Rink, 2013).

The regenerative power of planarians comes from the fact that neoblasts are pluripotent and can give rise to any cell type in the planarian (Elliott & Sánchez Alvarado, 2013; Rink, 2013). The importance of the neoblast population, and its pluripotency, was shown through a series of irradiation studies. Irradiating planarians, and thus destroying their neoblast population, ablates regenerative ability. Amazingly, a single neoblast cell is capable of rescuing an irradiating planarian (Elliott & Sánchez Alvarado, 2013). This suggests that neoblasts are the sole source of regenerative ability and a lack of regeneration indicates malfunction within the neoblast population. Conveniently, irradiation studies also provided characteristic phenotypes that can be used to identify neoblast malfunction. Lethal irradiation results in such characteristic phenotypes including “head regression, ventral curling and eventual lysis” (Rink, 2013).

Additionally, irradiation studies provide insight towards another facet of neoblast behavior: migration. Dividing neoblasts are absent from the pharynx and head region anterior to photoreceptors. In order to replace cells lost in these areas in which proliferation is absent, neoblasts rely on cell migration (Newmark & Sánchez Alvarado, 2000; Reddien & Alvarado, 2004). Interestingly, the movement of neoblasts is dependent upon injury and regeneration signals. If irradiation is applied without amputation, there is no rescue of the irradiated half of the animal and the irradiated half degenerates (Reddien & Alvarado, 2004). Together with studies on neoblast proliferation, this reveals that the blastema is formed through the combinative effort of cell migration and proliferation (Reddien & Alvarado, 2004).

## Cell Cycle

Regulation of stem cell proliferation is essential; excess proliferation can cause problems such as cancer and too little proliferation affects tissue maintenance, leading to premature aging (Rink, 2013). These activities of the cell that produce growth and proliferation are referred to as the cell cycle. The cell cycle is broken into two sections: interphase and mitosis. These two sections consist of four phases: $G_1$, S, $G_2$ and M. Mitosis makes up both a section and a phase, while $G_1$, $G_2$ and S are all considered phases of the section interphase (Cooper 2000). These phases contain a plethora of smaller processes that make up the larger four (Hartwell & Weinert, 1989). $G_1$ and $G_2$ refer to periods of 'gap' where the cell is preparing for a following phase. S phase consists of the synthesis (S) of DNA in preparation for producing the daughter cell. Finally, M phase consists of mitosis, and is completed by separation of the cells (Cooper 2000). These processes also serve as the checkpoints required to drive the cell cycle (Hartwell & Weinert, 1989).

The cell cycle is built upon levels of control. First, it is moderated by checkpoints, that "regulate fidelity of DNA replication and mitosis" (Masri, Cervantes, & Sassone-corsi, 2015). Forward progression is driven by these fixed, "switch-like" checkpoints, which are regulated by the cyclical expression of cyclins, protein translation and degradation, and phosphorylation. These processes are regulated co-dependent positive and negative feedback loops which regulate cell cycle checkpoints and create the cyclical oscillations of cell cycle factors. The cell cycle and many of its various control mechanisms are highly conserved throughout eukaryotes (Ferrell, 2013). Checkpoints allow the cell to monitor itself and its fidelity during the cell cycle, if inadequacies are detected a checkpoint, the cell cycle will not proceed and will instead pause to

correct any errors that would prove detrimental to the health of the cell (Hartwell & Weinert, 1989).

## Circadian Rhythms

Circadian rhythms form another cycling system in an organism. Circadian rhythms are endogenous biological processes within an organism that occur over approximately 24-hours (Peschel & Helfrich-Förster, 2011; Ünsal-Kaçmaz et al., 2005). The use of circadian rhythms gives an organism the ability to take in the context of countless environmental stimuli and patterns and respond in an advantageous way (Borgs et al., 2009; Masri et al., 2015; Mazzoccoli et al., 2016). Performing the correct function at the wrong time isn't helpful to the organism (Janich et al., 2013). In *Drosophila*, circadian rhythms underlie many important physiological and behavioral processes: "egg laying, pupal hatching (eclosion), adult locomotor activity, courtship, oviposition, endocrine activity, learning and memory abilities, oxygen consumption, as well as olfactory, gustatory, and visual sensitivity" (Mazzoccoli et al., 2016). Circadian timing is built upon a hierarchy of oscillators, some of which can be found in particular cell lines and even organs (Reppert & Wever, 2002). The first layer of this hierarchy is the concept of circadian 'clocks,' which are described by Mazzocoli et al. as a "cell-autonomous mechanism that regulates many biological processes as a function of the time of the day" (Mazzoccoli et al., 2016). The hierarchy begins at the 'master clock' and includes surrounding, usually referred to as peripheral, oscillators. The master clock is built from suprachiasmatic nuclei located in the hypothalamus. Here, exterior stimuli, such as light, direct the rhythmic outputs of the clock. The master clock uses these signals to coordinate its rhythmic outputs and direct peripheral oscillators (Reppert & Wever, 2002). The rhythms generated by this hierarchy are so robust that isolated cells continue their circadian oscillations in culture (Nagoshi et al., 2004).

The outputs of the clocks are a complex of genes and proteins that are rhythmically expressed in the organism and form feedback loops, therefore controlling rhythmic physiological or behavioral processes. The molecular foundation of the circadian clock is built by the core clock genes, which include: Clock (Clk), Cycle (Cyc), Period (Per), and Timeless (Tim) (Mazzoccoli et al., 2016; Reppert & Wever, 2002). These clock genes are expressed in a cyclical manner and create a temporal dimension that regulates the rhythmicity of the circadian cycle (Janich et al., 2013). Behind their cyclical expression is a system of feedback loops that function through transcriptional-translational control of circadian genes and their proteins (Mazzoccoli et al., 2016). Circadian rhythms are actually maintained by not one, but two feedback loops: one positive, one negative (Allada, 2003).

## Circadian Control of the Cell Cycle

The cycling of both the circadian rhythms and cellular processes of the cell are fundamentally similar: both the cell cycle and circadian clocks function based on the oscillation of genes, proteins and degradation that form autoregulatory feedback loops (Hunt & Sassone-Corsi, 2007). Because of these similarities and as additional roles for clock genes are discovered, emerging literature is suggesting a relationship between the cell cycle and circadian rhythms (Mazzoccoli et al., 2016). Idda et al. goes as far as to say that "one of the key outputs of the clock is the timing of cell cycle progression" (Idda et al., 2012). Notably, the eukaryotic cell cycle takes place over approximately one day (Hunt & Sassone-Corsi, 2007; Idda et al., 2012). Circadian oscillations persist throughout the process of cell division (Matsuo, Yamaguchi, & Mitsui, 2003; Nagoshi et al., 2004). Furthermore, cell cycle checkpoints and phases appear to be temporally controlled by the circadian clock (Borgs et al., 2009; Ünsal-Kaçmaz et al., 2005). One of the best examples of this is the temporal restriction of the S-phase transition in the cell

cycle, which occurs in the evening. While the mechanism behind this control remains ambiguous, it is hypothesized that synthesis is done at night, when exposure to UV damage from sunlight is lowest, in order to avoid DNA damage in a mechanistic phenomenon referred to as diapause (Idda et al., 2012; Janich et al., 2011; Masri et al., 2015; Mazzoccoli et al., 2016). Circadian control of S phase checkpoints has been demonstrated across multiple organisms (including humans and zebrafish) and tissue types (Geyfman & Andersen, 2010; Idda et al., 2012; Nagoshi et al., 2004). Clock genes display circadian rhythms in the skin (Geyfman & Andersen, 2010). Hair growth follows cyclic pattern of "growth, involution and rest" (Geyfman & Andersen, 2010). Clock genes were found to be associated with the hair growth cycle, particularly during specific transitions between phases where they regulate the timing and synchronization of these transitions (Geyfman & Andersen, 2010). The close relationship suggested between circadian rhythms and the cell cycle suggests mechanisms are in place between these two processes that allow for communication.

### ***Timeless* and *Timeout***

The confirmed role of the *timeless* gene is debated (Gotter et al., 2008; Ünsal-Kaçmaz et al., 2005). Classically, *timeless* is a vital component of circadian rhythms in *Drosophila melanogaster*, but the function of timeless in other organisms is less understood. While *Drosophila timeless* has importance to circadian rhythms in flies, there is no evidence of circadian effect in mammalian *timeless* (Clayton, Kyriacou, & Reppert, 2001; Mazzoccoli et al., 2016). Instead, identifications of *timeless* homologs in mice and humans appear to be more similar to a secondary gene in *Drosophila*, called *timeout*, and show an interesting similarity to a class of yeast proteins that are associated with cell cycle control (Chou & Elledge, 2006; Gotter et al., 2008; Masri et al., 2015; Ünsal-Kaçmaz et al., 2005). Interestingly, *timeout* is more

conserved than *timeless* throughout eukaryotes; and its non-circadian role has prompted a reevaluation of *timeless* (Gotter et al., 2008). Research reveals that *timeless* is a factor in cell cycle checkpoint regulations, having a role in S phase regulation through moderation of the combined efforts of the DNA damage response and DNA replication fork stability (Chou & Elledge, 2006; Gotter et al., 2008; Mazzoccoli et al., 2016).

Stress to the DNA of a cell initiates the DNA damage response checkpoint which in turn triggers stalling or cessation of the cell cycle through checkpoints in order to repair the damaged DNA before proceeding (Mazzoccoli et al., 2016). Ataxia telangiectasia mutated and Rad3-related protein (ATR) is a DNA damage-sensing protein that, along with Ataxia telangiectasia mutated (ATM), responds to DNA damage by phosphorylating checkpoint kinases to enact the cessation of the cell cycle (Benna et al., 2010; Borgs et al., 2009; Hunt & Sassone-Corsi, 2007; Mazzoccoli et al., 2016). *Timeless* is part of the ATR complex (Hunt & Sassone-Corsi, 2007; Mazzoccoli et al., 2016). Without *timeless*, ATR is not able to activate Checkpoint kinase 1 (Chk1) (Borgs et al., 2009; Ünsal-Kaçmaz et al., 2005). The pathway can be summarized as: ATR senses damage to the DNA, which activates Chk1. Chk1 phosphorylates downstream factors which halt the cell cycle and allow for repairs to occur (Mazzoccoli et al., 2016).

In both yeast and C. elegans, *timeless* and its' partner *tipin* protect stalled replication forks from collapsing. These forks have been stalled for DNA damage to be repaired (Gotter et al., 2008). The unwinding of the double helix during replication causes stress. Two physical processes, rotation of the fork and precatenation, follow behind the replication fork to compensate for this stress. DNA precatenanes are compressions of DNA that occur as DNA is being stabilized around the replication fork and the helix forms excess intertwinement. Should the stress on the DNA become too great, DNA replication will fail (Schalbetter et al., 2015).

*Timeless*, together with *Tipin*, actively constrain stress at the replication fork by moderating rotation and precatenation to ensure they proceed just far enough to prevent damage without compromising the efficiency of these two processes and DNA replication (Mazzoccoli et al., 2016; Schalbetter et al., 2015). Without the moderation of *timeless*, DNA damage, aneuploidy and cell cycle arrest can occur (Schalbetter et al., 2015). Depletion of *timeless* results in decreased replication integrity (Gotter et al., 2008).

# CHAPTER 3

# MATERIALS AND METHODS

Immunohistochemical staining protocol was adapted from the Forsthoefel, Waters and Newmark protocol to mark proliferating neoblasts (Forsthoefel et al., 2014). Some reagents were modified according to the results of multiple elimination analyses, in order to obtain specific and distinct staining results across our population of planarians. Feeding protocols were followed from the Rouhana et al. protocol (Rouhana et al., 2014). Confocal mosaic stitching protocols were adapted from the Microscopy Shared Resource Facility at the Icahn School of Medicine at Mount Sinai. ImageJ protocols were adapted from Larry Reinking from the Department of Biology at Millersville University.

## Planarian Stock Solution

A large 4 L beaker was filled with approximately 3.5 L of Millipore water. To this a solution of salts was added: 6.4 mL of 5M NaCl, 20 mL of 1M $MgSO_4$, 20 mL of 1M $CaCl_2$, 2 mL of 1M KCl and 2 mL of 1M $MgCl_2$. 2.02 g of $NaHCO_3$ was added as a buffer and the solution is mixed thoroughly until all $NaHCO_3$ is dissolved. The solution is then brought to a pH of 7.00 using 2N HCl. The final solution was brought up to 4 L using additional Millipore water and stored as a 5X solution. For use with the planarians for husbandry and experimental protocols, this solution was diluted to a 1X solution using Millipore water and labelled '1X Planarian Water'.

## Polymerase Chain Reaction (PCR)

Standard PCR protocol was followed using a 50 µL volume containing: 0.50 µL of a pGEM-T Easy Vector (Promega) with flanking T7 and SP6 promoter sequences plasmid template, 5 µL of 10X Dynazyme buffer, 0.5 µL of dNTPs at 25mM each, 1 µL each of T7

timeless forward and reverse primers, 0.5 µL of Taq Polymerase, and 41.50 µL of DEPC water. The thermocycler was set for 95˚C for 5 minutes, the following subset was completed 34 times: 94˚C for 30 seconds, 55˚C for 30 seconds, 72˚C for 1 minute and 15 seconds at 1 minute/1 kb), then 72˚C for 10 minutes and finally held at 4˚C.

## Purification of PCR Products

PCR products were purified using a PureLink™ PCR Purification Kit. 200 µL of Binding Buffer (B2) was added to 50 µL of the PCR product and mixed thoroughly. The sample was transferred to a Clean-up Spin Column, centrifuged for 1 minute, and then the flow-through was discarded. 650 µL of Wash Buffer (W1) was added to the column and centrifuged for 1 minute. The flow-through was again discarded and the column was centrifuged for 3 minutes to dryness. The column was then transferred to a clean 1.5 mL elution tube and 50 µL of Elution Buffer (E1) was added. This was incubated at room temperature for 1 minute, then followed with centrifugation for 1 minute. Agarose gel electrophoresis was used to verify the purified product.

## Agarose Gel Electrophoresis

To verify the purified product, 4 µL of the purified sample was transferred to a micro-centrifuge tube with 2 µL of loading dye. The sample was then vortexed and centrifuged. The 6 µL solution was pipetted into a well in a 1% agarose gel and run for 30 minutes. The results were compared to expected bands.

## In Vitro Transcription

In vitro transcription was used to transform DNA into dsRNA. A 20 µL solution was made using 2 µL of 10X Reaction Buffer, 2 µL of ATP solution, 2 µL of CTP solution, 2 µL of GTP solution, 2 µL of UTP solution, 4 µL of the PCR product. This was brought to 18 µL with RNase-free water. Finally 2 µL of Enzyme is added for the total 20 µL solution. This was

incubated at 37˚C for 4 hours. 1 µL of DNase was added, the solution was mixed and then incubated at 37˚C for 15 minutes. Lithium chloride was used to precipitate the RNA. 30µL of RNase-free water and 30 µL of lithium chloride was added to the solution. The same was mixed and held at -20˚C for 60 minutes. The sample was then centrifuged in 4˚C at maximum speed for 15 minutes. The resulting RNA pellet was resuspended in 40 µL of RNase-free water. To create the double-stranded RNA, a sample was placed in a PCR tube and run in a thermal cycler at 95˚C for 7 minutes, 75˚C for 5 minutes, 50˚C for 5 minutes, and 25˚C for 10 minutes. The final solution of dsRNA was stored at -20˚C until use for dsRNA feedings.

## Feeding Protocol

Dietary dsRNA was prepared using the Rouhana et al. protocol (Rouhana et al., 2014). Five planarians are aliquoted to two small Tupperware containers with 1X planarian water. In centrifuge tubes, 10 µL of calf liver was mixed with 2.5 µL of DEPC water for control animals, and 10 µL of calf liver was mixed with 1.95 µL of 0.770 ng/ µL *timeless* dsRNA construct and 0.55 µL of DEPC water for experimental animals. The centrifuge tubes are then ablated to mix the contents, and then condensed using centrifugation at 100,000 x for 10 seconds, three times. 10 µL of the resulting food pellet was pipetted into the containers for ingestion. The planarians were given 4-6 hours to ingest the food, confirmed by visual observation of the food in the digestive tract of an individual animal. After feeding, the water of the containers was changed and the planarians were replaced in the 21ºC incubator. Feedings were conducted three times in one week: Monday, Wednesday, and Friday.

## Amputation

Worms were amputated approximately 72 hours after the final feeding. A single worm was pipetted onto a microscope slide and amputated into three fragments using a straight razor

blade. Amputated fragments were then incubated in small Tupperware cups in 1X planarian water at 21ºC for 48 hours in preparation for immunohistochemical staining.

## Staining Protocol

The immunohistochemical stain protocol was adapted from (Forsthoefel et al., 2014), and completed over the course of 4 experimental days. To begin the staining protocol, solutions were made and 5.5% HCl, Carnoy's, and methanol were placed in ice to chill. On the first day, whole animals or fragments were transferred into scintillation vials and placed on ice for approximately 2 minutes, or until the movement of the animals was reduced. The 1X planarian water was decanted out of scintillation vials and replaced with 10 µL of ice-cold HCl in each vial. The vials were vigorously shaken for 3 minutes, followed by immediate removal of the HCL and replacement with 10 µL of the ice-cold Carnoy's fixative solution in each vial. During this step, the vials were gently agitated by hand to prevent the animals from adhering to one another or the vials. The vials with Carnoys were placed on a nutator in 4˚C to fix for two hours. After fixation, the Carnoys solution was decanted and replaced with 10 µL of ice-cold methanol to was the animals for 10 minutes. At this point, the experiment could be held over the weekend in preparation to continue the stain. On continuation of the stain, the planarians were rehydrated using a 50:50 methanol:PBSTx solution and washed for 10 minutes, followed by two 5 minute washes of PBSTx. For bleaching, the PBSTx was replaced with bleach and allowed to sit overnight at room temperature under incandescent lighting. Following rehydration, animals were removed from scintillation vials containing the bleach and placed in centrifuge tubes. They were then rinsed in PBSTx two times, then washed in PBSTx for ten minutes twice. Animals were blocked in 1% BSA solution for two hours. Then, 0.950 mL of Millipore anti-phospho-histone H3 anti-horseradish peroxidase primary antibody was added to each tube, with a concentration of

1:500. Animals were then incubated overnight at room temperature on a nutator. Next, the planarians were rinsed two times in PBSTx and then washed for two hours with at least six changes of the solution. After washing, 0.950 mL of Jackson goat anti-rabbit anti-horseradish peroxidase secondary at a concentration of 1:200 was aliquoted into the two tubes. This was again incubated overnight at room temperature on a nutator. The final day of the stain consists of washing and tyramide signal amplification. Planarians were again rinsed two times in PBSTx and then washed for two hours with at least six changes of solution. Animals were placed 1 mL of 1:500 concentration house-made tyramide and PBSTx mixture. The tubes were then covered with foil to protect the tyramide from premature excitation. Tubes were nutated at room temperature for ten minutes and then 33μL of a 1% hydrogen peroxide mixture was added to each tube. After an additional thirty minutes, the tyramide and hydrogen peroxide solution was removed. The covered tubes were washed for one hour on a nutator at room temperature with at least three changes in solution and then stored at 4˚C, while nutating, over the weekend in fresh PBSTx. For final storage, the PBSTx is replaced with a 90% glycerol solution and 1 drop of Vectashield with DAPI.

**Tyramide Signal Amplification Construction**

Tyramide signal amplification protocol from (King & Newmark, 2013) was used to produce house-made tyramide. A tyramine stock was made by mixing tyramine hydrochloride in anhydrous N,N-Dimethylformamide (DMF) with 10 μl/ml triethylamine until the final concentration was 10mg/ml. Additionally, a flour-conjugated (Dye-)NHS ester was made by adding 5/6 carboxyflourescein succinimidyl ester (FAM) to DMF until it reached a final concentration of 10mg/ml and incubated at room temperature for 2 hours in darkness. Next, 100mg of the Dye-NHS solution was combined with 3,425 μl of the 10 mg/ml tyramine solution

and diluted with 86 ml of ethanol. The resulting tyramide solution was aliquoted into 2 ml centrifuge tubes and stored at -20˚C.

## Imaging

Specimens were placed on a clean microscope slide in 3-4 drops of storage 90% glycerol/Vectashield/DAPI solution with a coverslip. Specimens were then viewed using the Fluoview 1000V confocal microscope. Specimens were located using the trans lamp and 10x magnification. After location, the stain was viewed using the Fluoview Version 3.1 software. Fragments are centered into view, still using 10x magnification, and lasers for alexa-488 and DAPI are adjusted for a bright image without excess saturation. HV, Gain and Offset are adjusted to ranges of 400-600, 0-2, and 0-3, respectively. Once the settings were adjusted, the images were then optically sectioned using the z-stack function. The depth of the stack was selected according to the lowest and highest z positions in which neoblasts could be seen. This was then divided into 10-12 sections. The confocal then proceeded to take 10-12 images at each optical section and the resulting images are stacked for a z projection. For quantification purposes, the z-projections were saved with one combined alexa-488/DAPI and one alexa-488 stain as .TIF images.

## Mosaic Stitching

For whole animals, a mosaic stitching protocol must be used in order to obtain an image of the entire specimen. After location of the specimen, settings were adjusted according to the above protocol. The multi area time lapse function is used. A custom mosaic outline is selected and the outer perimeter of the animal is mapped and added to the registered point list. A short experiment is run without z-stack parameters to check the mosaic image and ensure that the entire animal has been captured by the outline. If acceptable, the experiment is then run using the

following z-stack parameters. The depth of the z-stack is selected by the lowest and highest depths in which neoblasts can be seen and a clear outline of the animal is visible. This is then divided into a larger range of sections than animals that have been amputated, due to the variation of 'thicknesses' among whole animals and resulting position in glycerol beneath the coverslip. Specimens were optically sectioned into 15-31 z-stack sections. The mosaic stitching protocol is then run using a concurrent z-stack protocol. The complete mosaic is checked for an accurate representation of the specimen's outline and neoblast topography through each section and then saved as an .OIF file. This file is used to obtain the z projection of the mosaic and the images can again be saved as combined alexa-488/DAPI and alexa-488 stain .TIF images for quantification purposes.

**ImageJ**

Confocal images were uploaded as .TIF files into the ImageJ 1.51k software. For regeneration studies (fragments), Alexa-488 images were converted to 8-bit, and the threshold was adjusted for a light background and contrasted neoblasts. Neoblasts were counted using analyze particles function. To identify the size range of neoblasts, a sample diameter was taken using the straight-line tool across the smallest and largest identified neoblasts. These measurements were then used to identify neoblasts as particles to be counted with an average range of 7-12 pixels in diameter and a circularity of 0-5. The resulting masked image contained outlines of each counted particle and the summary provided particle count. The mask image was also visually compared to the original Alexa-488 image in order to ensure that the topography of neoblasts was accurately represented in the count. To find the area of both whole animals and fragments, the combined Alexa-488 and DAPI images were converted to 8-bit, and the threshold was adjusted for a light background and a completely saturated threshold area for the body of the

animal. Using the 500 µm scalebar, image calculations were scaled to pixels/millimeter. Once the scale was set to millimeters, the outline of the animal is obtained using the freeform lasso tool or the rectangle tool (both produce the same quantification of area) and the measure tool was selected. This calculation resulted in the area of the saturated animal being quantified and reported in the summary (in $mm^2$).

### Statistical Analysis of Neoblast Quantification

Neoblast quantifications and the area of each planarian or fragment were gathered using ImageJ calculations. Statistics were obtained using Office Excel 2016. The number of neoblasts were averaged over the area of the animal to account for any variation in the size of amputated fragments or whole planarians. For amputated fragments, if the planarian was too large to calculate the area, the sample was discarded. The number of neoblasts per area ($mm^2$) were calculated for each planarian, and this number was averaged across all control and all timeless-treated planarians in one experimental group to be counted as one repetition. Individual planarians were treated as subsamples. These parameters were used for both regeneration (fragments) and whole animal studies. From these results, a single-factor ANOVA was run for both whole animal and regeneration studies using an alpha value of 0.5.

# CHAPTER 4

# RESULTS

## Optimization of Immunohistochemical Stain

Previous results in the laboratory produced stains that were non-specific with high background, and initial attempts to strengthen the stain proved too rigorous and compromised tissue integrity. Over the course of approximately one year, multiple elimination studies were performed for each step of the immunohistochemical staining process: sacrifice and mucus removal, fixation, reduction, bleaching, primary and secondary antibodies, and tyramide signal amplification. The current protocol was developed as a result of these elimination studies and provides a punctate, specific stain with minimized background, and minimal effects to tissue integrity. Using the current protocol, neoblast specific PH3+ fluorescent staining was confirmed using light microscopy and comparing our results to the expected size, shape and locality (posterior to photoreceptors) of typical neoblasts (Figure 2).

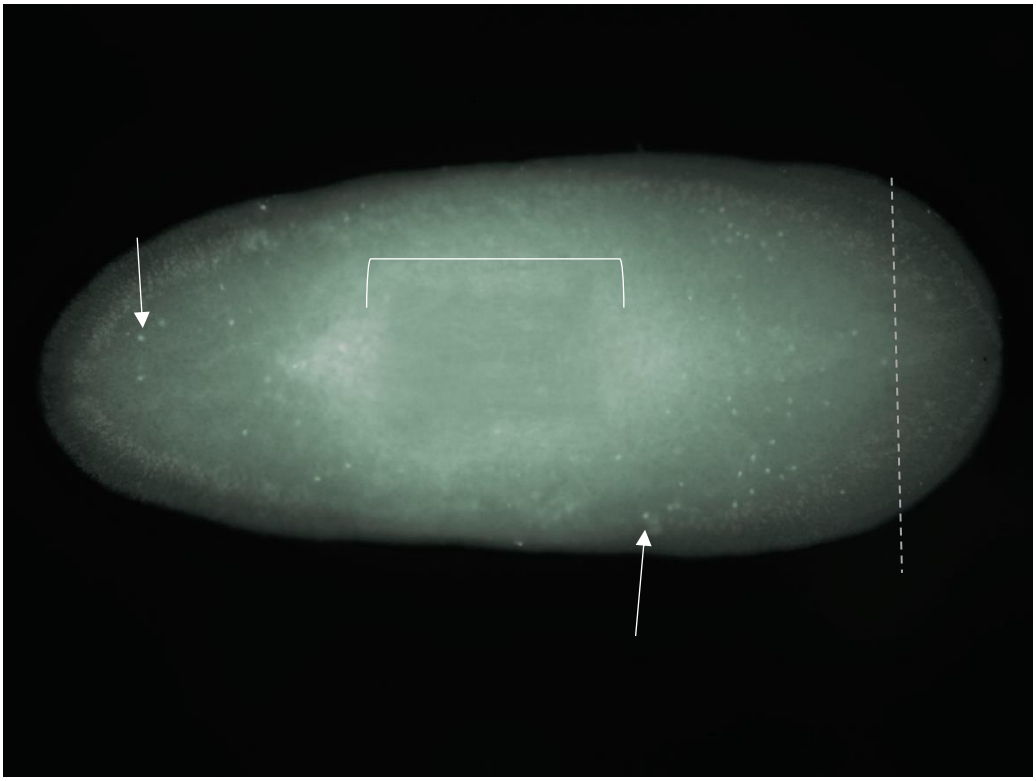

*Figure 2*. Image of neoblasts in a whole planarian obtained using Zeiss microscope. Mitotic neoblasts stained using PH3+ are indicated with white arrows. A dashed line is drawn across the photoreceptors to indicate the region anterior to the photoreceptors that is devoid of proliferating neoblasts. The pharynx is indicated with a white bracket.

**dsRNA Construction**

PCR was run using the plasmid, and *in vitro* transcription was used to acquire a dsRNA (Figure 3). We confirmed the PCR product using agarose electrophoresis gel. We determined the concentration using a NanoDrop microvolume spectrophotometer to be 770 ng/mL.

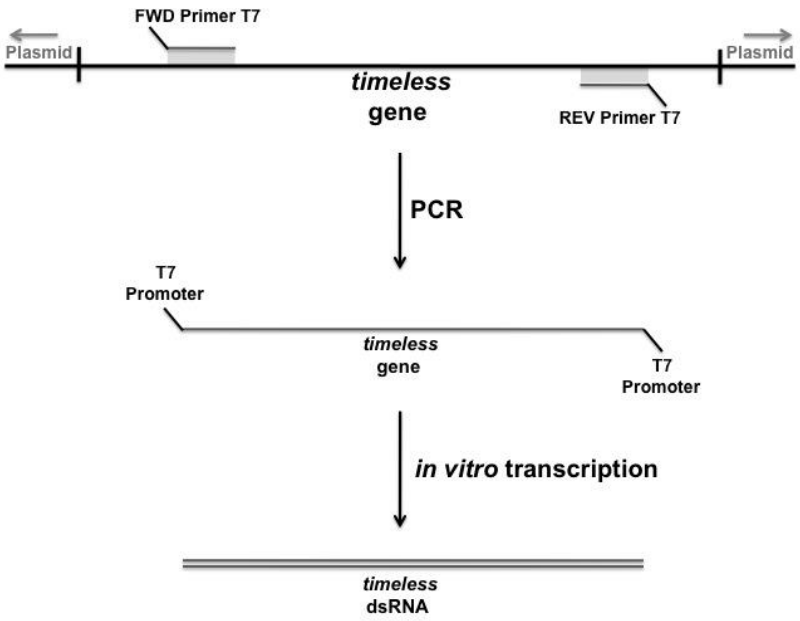


*Figure 3*. Polymerase chain reaction to dsRNA construction. PCR was used to amplify timeless gene sequence and *in vitro* transcription to create the dsRNA product at a concentration of 770ng/mL.

## dsRNA Interference and Immunohistochemistry

We targeted the function of the *timeless* gene by adding our 770 ng/mL dsRNA construct to the planarian diet. Five worms of similar size were collected for each experimental group and fed either a dsRNA diet mixture or control diet mixture three times over the course of one week. For regeneration studies, planarians were amputated via trisection 72 hours after the final feeding. These fragments were then immunohistochemically stained 48 hours after amputation using phospho-histone H3 as a marker for mitotic neoblasts (Figure 4 & 5). For whole-animal studies, planarians were fed following the same feeding guidelines and immunohistochemically stained using phospho-histone H3 as a marker for mitotic neoblasts 5 days (120 hours) after the final feeding (Figure 6 & 7).

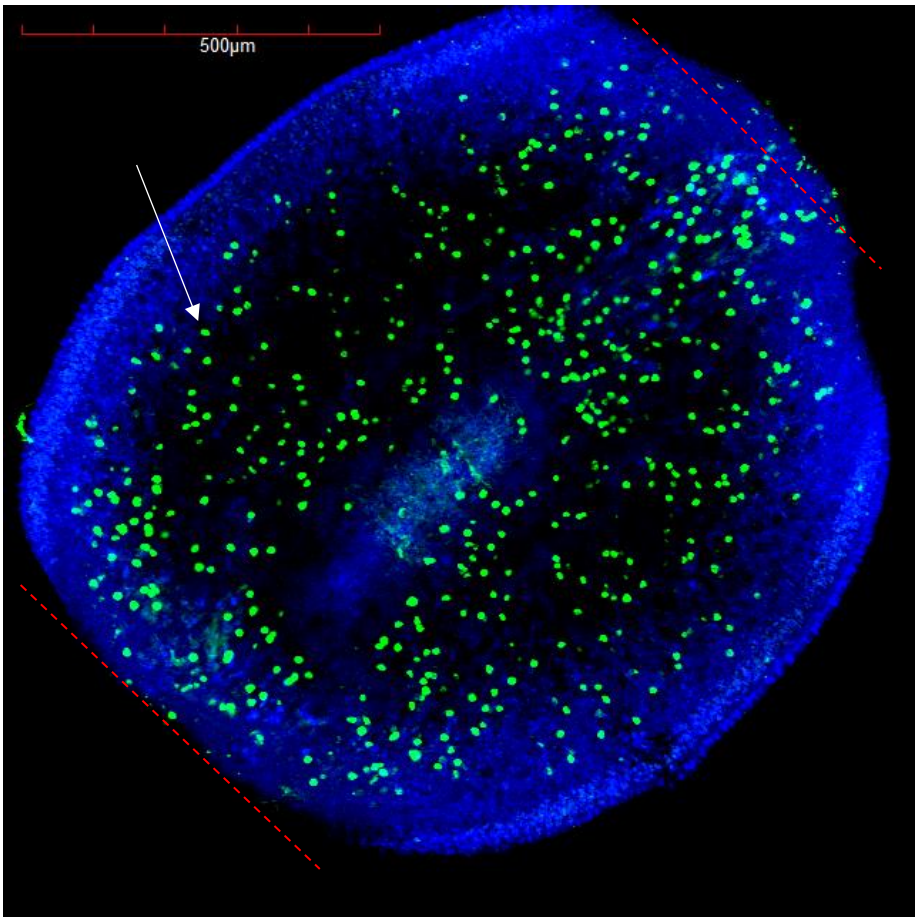


*Figure 4*. Immunohistochemical phospho-histone H3 stain in an amputated fragment (control). Mitotic neoblasts are visible as green fluorescent spheres in the amputated fragment, indicated by white arrows. Dividing neoblasts are fluorescently labelled with Alexa-488, using phospho-histone H3 as a label for mitotic activity. DAPI was used as a background stain, visible as the blue area of the fragment. The region of amputation is marked using red dashed lines. Scale bar 500 µm in the top left corner.

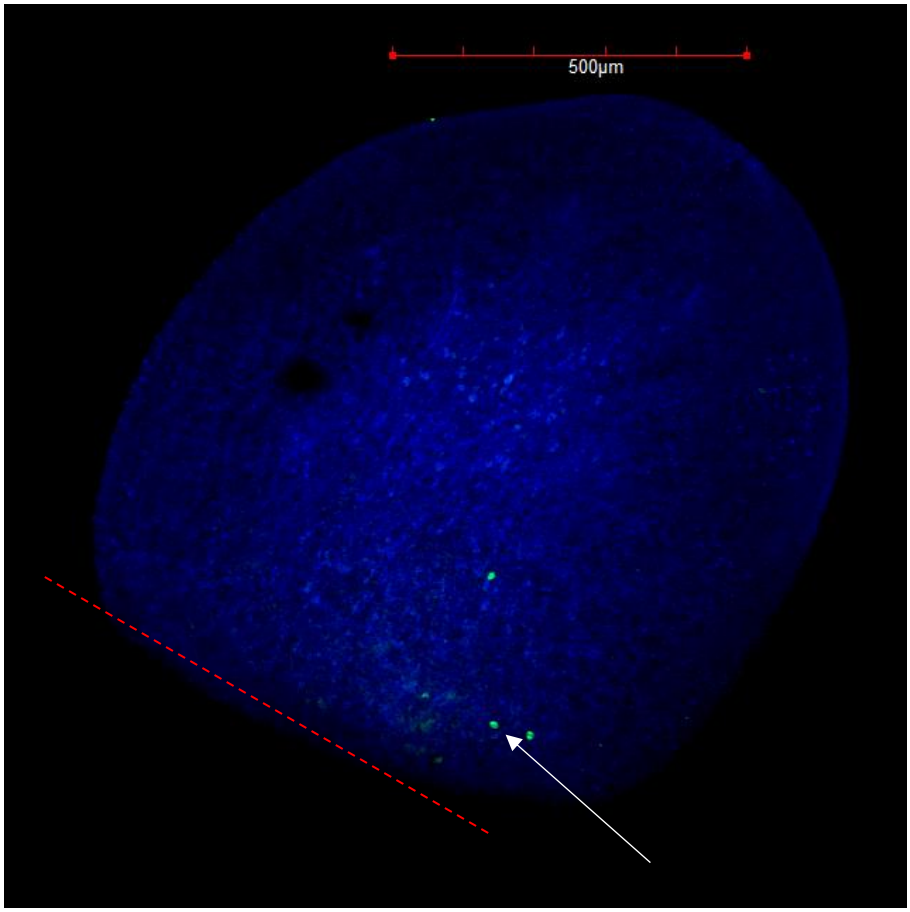


*Figure 5*. Immunohistochemical phospho-histone H3 stain in an amputated fragment (*timeless* dsRNA treated). Mitotic neoblasts are visible as green fluorescent spheres in the amputated fragment, indicated by white arrows. Dividing neoblasts are fluorescently labelled with Alexa-488, using phospho-histone H3 as a label for mitotic activity. DAPI was used as a background stain, visible as the blue area of the fragment. The region of amputation is marked using red dashed lines. Scale bar 500 µm in the top right corner.

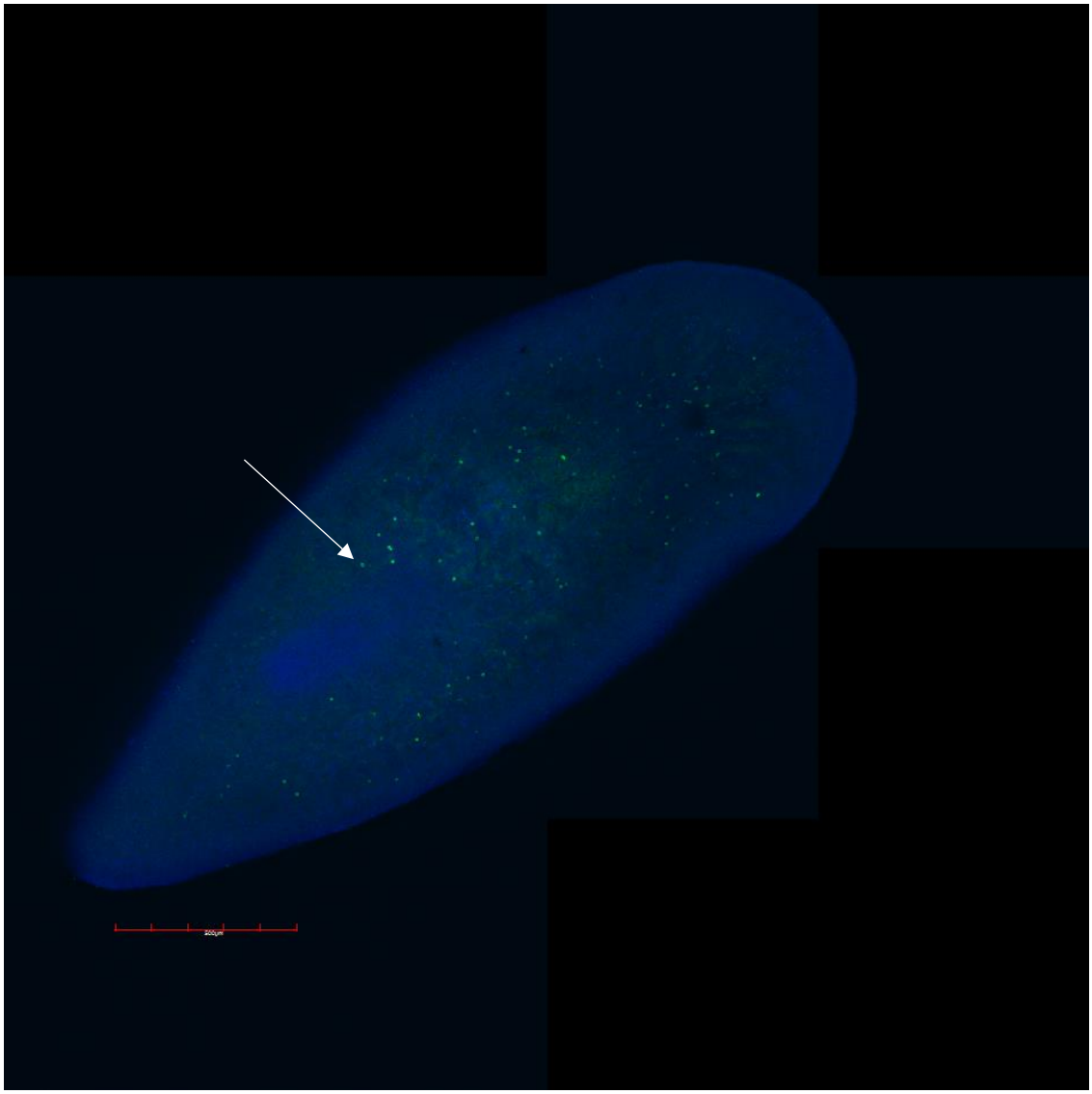

*Figure 6.* Immunohistochemical phospho-histone H3 stain in a whole planarian (control). Mitotic neoblasts are visible as green fluorescent spheres, indicated by white arrows. Dividing neoblasts are fluorescently labelled with Alexa-488, using phospho-histone H3 as a label for mitotic activity. DAPI was used as a background stain, visible as the blue area of the animal. Scale bar 500 μm in the bottom left corner.

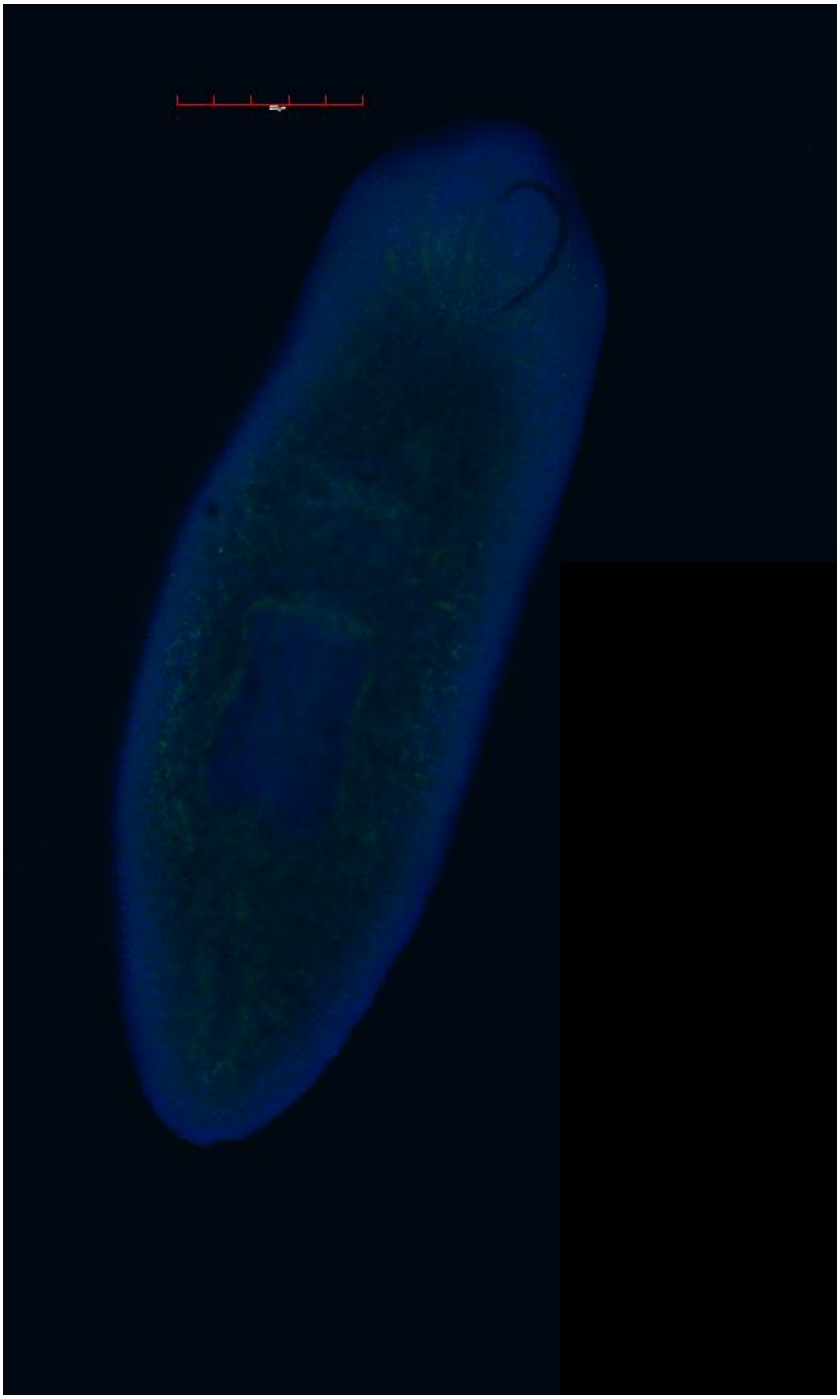

*Figure 7.* Immunohistochemical phospho-histone H3 stain in a whole planarian (*timeless* dsRNA treated). Mitotic neoblasts are visible as green fluorescent spheres, indicated by white arrows. Dividing neoblasts are fluorescently labelled with Alexa-488, using phospho-histone H3 as a label for mitotic activity. DAPI was used as a background stain, visible as the blue area of the animal. Scale bar 500 μm in the top left corner.

## Quantification of Mitotic Neoblasts

We quantified mitotic neoblasts using the ImageJ version 1.51k software. Images obtained from confocal microscopy were uploaded into ImageJ as .TIF images and were converted to 8-bit, where the threshold could be adjusted to produce contrasted images of neoblasts (Figure 8). These adjusted images could then be analyzed based on threshold contrast using the "Analyze Particles" function. Using outlines to identify each individual neoblast, the neoblast 'map' could be compared to the original stained image to compare neoblast 'topography' and ensure an accurate count of represented neoblasts (Figure 9 A and B). The summary provided by ImageJ includes the number of neoblasts and was transferred into Office Excel 2016. Neoblast quantities were converted into neoblast per millimeter by averaging the number of neoblasts across the area of the planarian or fragment. These numbers were averaged across control and *timeless*-treated animals or fragments, which were recorded as subsamples in a larger repetition. Each experiment was recorded as one repetition, for a total of three repetitions. We ran a one-factor ANOVA with Excel using an alpha value of 0.5. For regeneration studies, we obtained a significant p-value of 0.01 (Figure 10). The same one-factor ANOVA with Excel using an alpha value of 0.5 was run for whole animal studies and obtained a significant p-value of 0.03 (Figure 11).

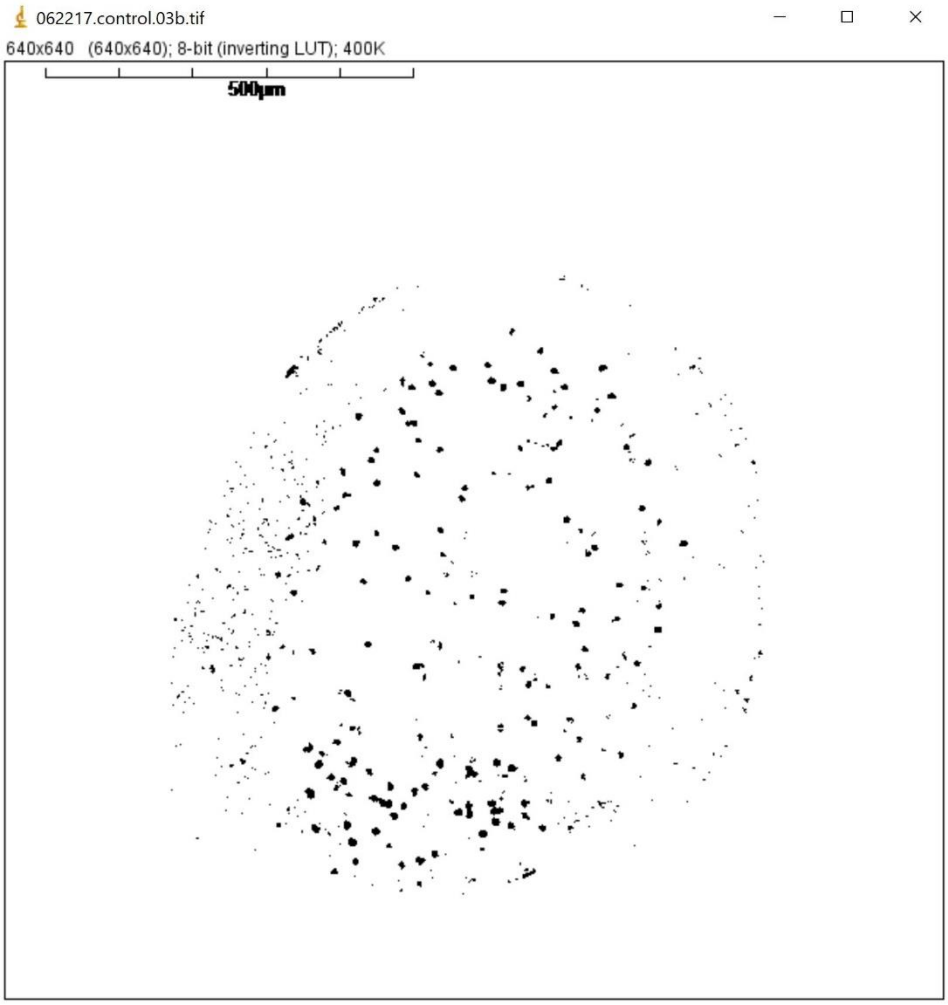


*Figure 8*. Neoblast image with adjusted threshold. An 8-bit image threshold was adjusted until the background was white and neoblasts were completely contrasted in order to be counted using the “Analyze Particles” function.

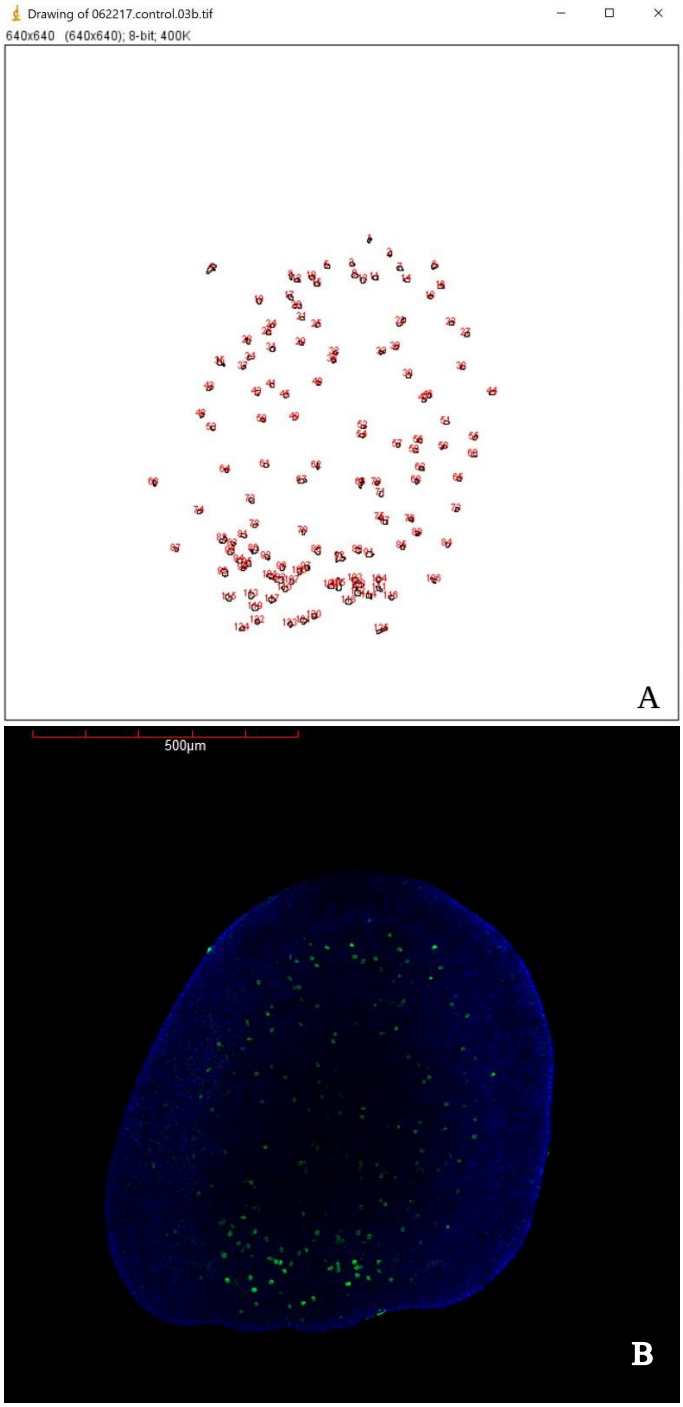


*Figure 9.* ImageJ neoblast quantification map. Generated neoblast map with numbered and outlined neoblasts, (A), is compared to the original combined stain image, (B), to ensure accurate representation of neoblast topography.

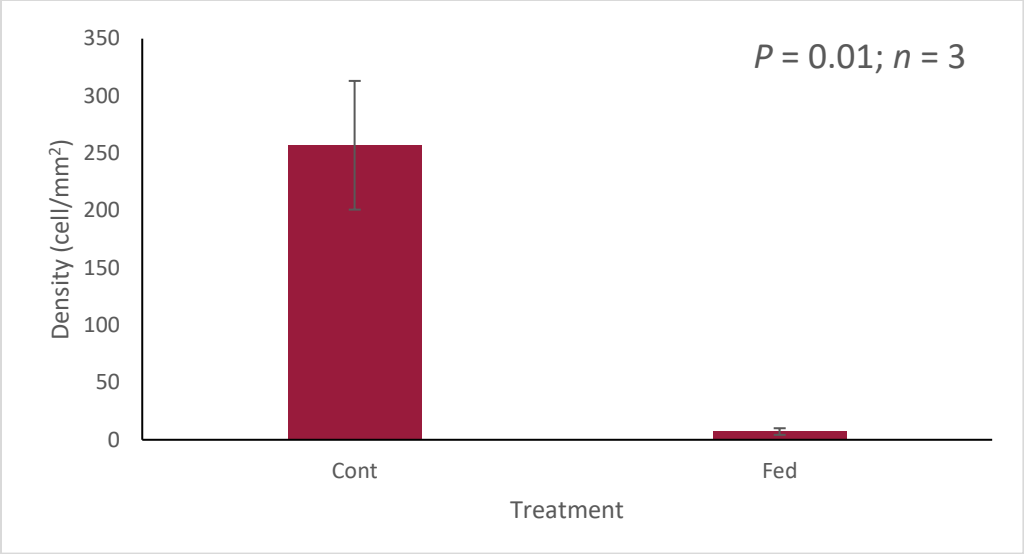


*Figure 10*. Neoblast quantification of amputated fragments. The average number of neoblasts per $mm^2$ between control (Cont) and *timeless*-treated (Fed) is significantly reduced in treated planarian fragments (p-value 0.01) n=3. Bars represent average number of neoblasts per $mm^2$ of area, with standard error bars.

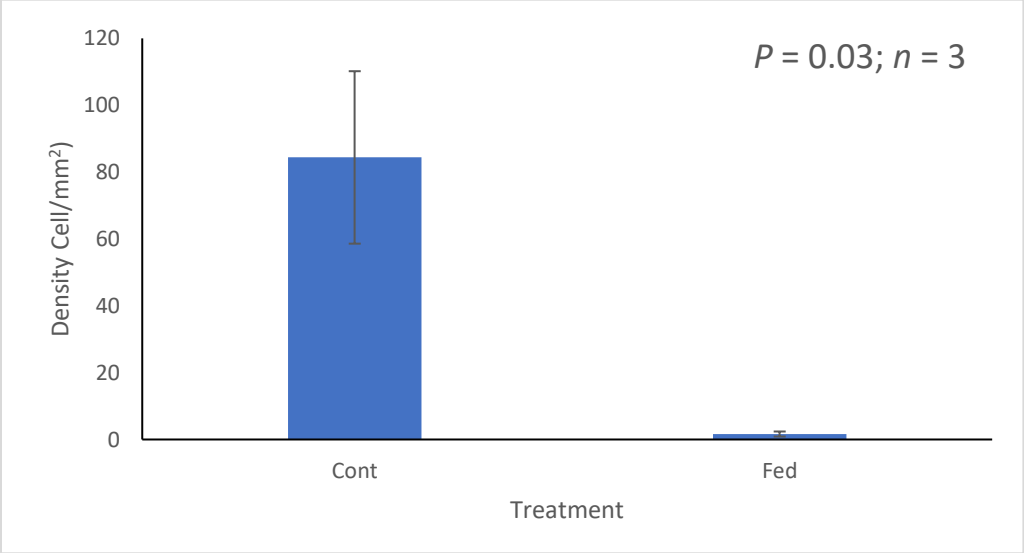


*Figure 11*. Neoblast quantification of whole animals. The average number of neoblasts per $mm^2$ between control (Cont) and *timeless*-treated (Fed) is significantly reduced in treated planarians (p-value 0.03) n=3. Bars represent average number of neoblasts per $mm^2$ of area, with standard error bars.

# CHAPTER 5

# DISCUSSION

Regeneration is an important human health concern (Nakada et al., 2011; Poss, 2002; Ünsal-Kaçmaz et al., 2005). A lack of regeneration in vital tissues severely limits regenerative capabilities, as well as normal tissue maintenance (Nakada et al., 2011; Poss, 2002). The inability to combat these limitations can cause DNA damage, cancer and disease (Mazzoccoli et al., 2016; Nakada et al., 2011). As human medicine investigates the mechanisms behind regeneration, it has become clear that circadian clock and the cell cycle are intertwined through the process of proliferation– but the exact factors, or even pathways, are still debated (Mazzoccoli et al., 2016; Ünsal-Kaçmaz et al., 2005).

The mechanisms behind regeneration are still unclear. Previous results in Dr. Major's laboratory revealed that when *timeless* is targeted using RNAi, no blastema is formed. This characteristic phenotype is specifically associated with neoblast malfunction, and indicates that regeneration is not taking place (Rink, 2013). This suggests that *timeless* is required for planarian regeneration. My thesis aimed to characterize the role of *timeless* in planarian regeneration and learn more about the mechanisms that are required for regeneration. My results on mitotic neoblast quantification indicate a significant decrease in the number of proliferating neoblasts in *timeless* dsRNA-treated planarians, as compared to controls. This is true in both amputated animals, where neoblasts are dividing to form a blastema and regenerate, and in whole animals, where neoblasts are dividing to drive physiological tissue maintenance. All together this indicates that *timeless* is required for neoblast proliferation and raises interesting questions regarding a circadian control input in the regeneration process.

While it may seem unusual for a clock gene to be involved in regeneration, emerging literature continues to find evidence of circadian control of cellular processes. As described previously, there is a strong relationship between the circadian clock and the cell cycle (Borgs et al., 2009; Idda et al., 2012; Ünsal-Kaçmaz et al., 2005). Most notably, through the temporal restriction of S phase during the cell cycle (Idda et al., 2012; Janich et al., 2011; Masri et al., 2015; Mazzoccoli et al., 2016). However, there are also examples of circadian control over stem cells. In murine hematopoietic stem cells, circadian rhythms control mobilization of stem cells from the bone marrow into the circulating blood (Lucas et al., 2008). In hair follicles, which harbor stem cells, the CLOCK controls gene expression that produces a cyclical hair growth cycle that oscillates in a circadian manner (Geyfman & Andersen, 2010; Lin et al., 2009). Similarly, human epidermal stem cells display gating of cell cycle phases and cellular activities dependent on peaks in circadian oscillations. Cell cycle phases are gated over a 24 hour period, temporally divided into specific intervals that are defined by cellular processes contained within these intervals (Janich et al., 2013).

Strikingly, there is also emerging evidence of circadian control over regeneration processes. Zebrafish have the ability to regenerate their fins following amputation. There are robust circadian rhythms in the fin, and these rhythms control the cell cycle and proliferation in this area. Following injury to the fin, circadian-driven proliferation increases. Most importantly, this proliferative response is gated by circadian rhythms. Particularly in the fin, proliferation following injury does not follow a fixed rhythmicity, but rather, reflects a dependence on the time of injury. Proliferation, specifically S phase, is temporally restricted to the evening, suggesting again that these processes may be confined to times when UV exposure will be at its lowest during a 24-hour period (Idda et al., 2012).

These results strongly support circadian control over the cell cycle, stem cells and regeneration. Understanding the mechanisms that underlie this process will continue to provide therapeutic tactics that may support a more efficient regeneration response. As suggested by Ünsal-Kaçmaz et al., Timeless may act as a direct factor between regeneration, cell cycle regulation, and the circadian clock, facilitating communication and feedback between these processes (Ünsal-Kaçmaz et al., 2005). We hypothesize that timeless acts as the communication link between these processes and that this dual role allows timeless to control neoblast proliferation, thereby controlling the regeneration response.

## Future Directions

Our definition of clock genes is still evolving. Historically, heterozygous mutants of mammalian *timeless* do not display a disruption in circadian rhythms, leading to its rejection as a canonical clock gene. Describing the planarian *Timeless* gene and its role in circadian rhythms will add to the understanding of circadian mechanisms behind the cell cycle. It may be that the planarian *timeless* gene is also closer to the *Drosophila* gene *timeout* and may only have a role in cell cycle control (Ünsal-Kaçmaz et al., 2005). Phylogenetic studies could be used to determine the origins of planarian *timeless*, and its relatedness to Drosophila *timeless* and *timeout*. This could be coupled with circadian rhythm studies to evaluate if there is a circadian rhythmicity to regeneration and if rhythmicity is affected when *timeless* is targeted. Finally, BrdU labelling may provide insight into the exact phase of the cell cycle in which timeless is involved. It is plausible that timeless is involved in S phase, due to the relationship between timeout and S phase processes, but also due to the fact that the timeless protein is accumulated during the evening, where S phase appears to be temporally restricted.

References

Allada, R. (2003). Circadian Clocks: A tale of two feedback loops. *Cell*, *112*(3), 284–286. doi:10.1016/S0092-8674(03)00076-X

Bell, D. R., & Van Zant, G. (2004). Stem cells, aging, and cancer: Inevitabilities and outcomes. *Oncogene*, *23*(43 REV. ISS. 6), 7290–7296. doi:10.1038/sj.onc.1207949

Benna, C., Bonaccorsi, S., Wülbeck, C., Helfrich-Förster, C., Gatti, M., Kyriacou, C. P., … Sandrelli, F. (2010). Drosophila timeless2 is required for chromosome stability and circadian photoreception. *Current Biology*, *20*(4), 346–352. doi:10.1016/j.cub.2009.12.048

Borgs, L., Beukelaers, P., Vandenbosch, R., Belachew, S., Nguyen, L., & Malgrange, B. (2009). Cell circadian cycle: New role for mammalian core clock genes. *Cell Cycle*, *8*(6), 832–837. doi:10.4161/cc.8.6.7869

Chou, D. M., & Elledge, S. J. (2006). Tipin and Timeless form a mutually protective complex required for genotoxic stress resistance and checkpoint function. *Proceedings of the National Academy of Sciences of the United States of America*, *103*(48), 18143–18147. doi:10.1073/pnas.0609251103

Clayton, J. D., Kyriacou, C. P., & Reppert, S. M. (2001). Keeping time with the human genome. *Nature*, *409*(6822), 829–831. doi:10.1038/35057006

Danielle Wenemoser; Peter W. Reddien. (2011). Planarian regeneration involves distinct stem cell responses to wounds and tissue absence. *Developmental Biology*, *344*(2), 979–991. doi:10.1016/j.ydbio.2010.06.017.Planarian

Elliott, S. A., & Sánchez Alvarado, A. (2013). The history and enduring contributions of planarians to the study of animal regeneration. *Wiley Interdisciplinary Reviews: Developmental Biology*, *2*(3), 301–326. doi:10.1002/wdev.82

Ferrell, J. E. F. J. (2013) Feedback loops and reciprocal regulation: Recurring motifs in the systems biology of the cell cycle. *Current Opinion Cell Biology*, *25*(6), 1–21. doi:10.1016/j.ceb.2013.07.007.Feedback

Forsthoefel, D. J., Waters, F. A., & Newmark, P. A. (2014). Generation of cell type-specific monoclonal antibodies for the planarian and optimization of sample processing for immunolabeling. *BMC Developmental Biology*, *14*, 1–22. doi:10.1186/s12861-014-0045-6

Geyfman, M., & Andersen, B. (2010). Clock genes, hair growth and aging. *Aging*, *2*(3), 122–128. doi:10.18632/aging.100130

Gotter, A. L., Suppa, C., & Emanuel, B. S. (2008). Mammalian TIMELESS and Tipin are evolutionarily conserved replication fork-associated factors. *Journal of Molecular Biology*, *6*(9), 2166–2171. doi:10.1021/nl061786n.Core-Shell

Hartwell, L. H., & Weinert, T. A. (1989). Checkpoints : Controls that ensure the order of cell cycle events. *Science*, *246*, 629–634. doi:10.1126/science.2683079

Hunt, T., & Sassone-Corsi, P. (2007). Riding tandem: Circadian clocks and the cell cycle. *Cell*, *129*(3), 461–464. doi:10.1016/j.cell.2007.04.015

Idda, M. L., Kage, E., Lopez-Olmeda, J. F., Mracek, P., Foulkes, N. S., & Vallone, D. (2012). Circadian timing of injury-induced cell proliferation in zebrafish. *PLoS ONE*, *7*(3). doi:10.1371/journal.pone.0034203

Janich, P., Pascual, G., Merlos-Suárez, A., Batlle, E., Ripperger, J., Albrecht, U., … Benitah, S. A. (2011). The circadian molecular clock creates epidermal stem cell heterogeneity. *Nature*, *480*(7376), 209–214. doi:10.1038/nature10649

Janich, P., Toufighi, K., Solanas, G., Luis, N. M., Minkwitz, S., Serrano, L., … Benitah, S. A. (2013). Human epidermal stem cell function is regulated by circadian oscillations. *Cell Stem*

*Cell*, *13*(6), 745–753. doi:10.1016/j.stem.2013.09.004

King, R. S., & Newmark, P. A. (2013). In situ hybridization protocol for enhanced detection of gene expression in the planarian Schmidtea mediterranea. *BioMed Central Developmental Biology*, *13*(1). doi:10.1186/1471-213X-13-8

Lin, K. K., Kumar, V., Geyfman, M., Chudova, D., Ihler, A. T., Smyth, P., … Andersen, B. (2009). Circadian clock genes contribute to the regulation of hair follicle cycling. *Public Library of Science Genetics*, *5*(7). doi:10.1371/journal.pgen.1000573

Liu, S. Y., Selck, C., Friedrich, B., Lutz, R., Vila-Farré, M., Dahl, A., … Rink, J. C. (2013). Reactivating head regrowth in a regeneration-deficient planarian species. *Nature*, *500*(7460), 81–84. doi:10.1038/nature12414

Lucas, D., Battista, M., Shi, P. A., Isola, L., & Frenette, P. S. (2008). Mobilized hematopoietic stem cell yield depends on species-specific circadian timing. *Cell Stem Cell*, *3*(4), 364–366. doi:10.1016/j.stem.2008.09.004

Masri, S., Cervantes, M., & Sassone-corsi, P. (2015). The circadian clock and cell cycle: Interconnected biological circuits. *Current Opinion Cell Biology*, *25*(6), 730–734. doi:10.1016/j.ceb.2013.07.013

Matsuo, T., Yamaguchi, S., & Mitsui, S. (2003). Control mechanism of the circadian clock for timing of cell division in vivo, *302*(October), 255–259. doi:10.1126/science.1086271

Mazzoccoli, G., Laukkanen, M. O., Vinciguerra, M., Colangelo, T., & Colantuoni, V. (2016). A timeless link between circadian patterns and disease. *Trends in Molecular Medicine*, *22*(1), 68–81. doi:10.1016/j.molmed.2015.11.007

Nagoshi, E., Saini, C., Bauer, C., Laroche, T., Naef, F., & Schibler, U. (2004). Circadian gene expression in individual fibroblasts: Cell-autonomous and self-sustained oscillators pass

time to daughter cells. *Cell*, *119*(5), 693–705. doi:10.1016/j.cell.2004.11.015

Nakada, D., Levi, B. P., & Morrison, S. J. (2011). Integrating physiological regulation with stem cell and tissue homeostasis. *Neuron*, *70*(4), 703–718. doi:10.1016/j.neuron.2011.05.011

Newmark, P. A., & Sánchez Alvarado, A. (2000). Bromodeoxyuridine specifically labels the regenerative stem cells of planarians. *Developmental Biology*, *220*(2), 142–153. doi:10.1006/dbio.2000.9645

Pearson, B. J., & Sánchez Alvarado, A. (2009). Regeneration, stem cells, and the evolution of tumor suppression regeneration. *Cold Spring Harbor Symposia on Quantitative Biolog*, *LXXIII*, 565–572. doi:10.1101/sqb.2008.73.045

Peschel, N., & Helfrich-Förster, C. (2011). Setting the clock - by nature: circadian rhythm in the fruitfly Drosophila melanogaster. *Federation of European Biochemical Societies Letters*, *585*(10), 1435–1442. doi:10.1016/j.febslet.2011.02.028

Poss, K. D. (2002). Heart regeneration in zebrafish supplemental. *Science*, *298*(5601), 2188–2190. doi:10.1126/science.1077857

Reddien, P. W., & Alvarado, A. S. (2004). Fundamentals of planarian regeneration. *Annual Review of Cell and Developmental Biology*, *20*(1), 725–757. doi:10.1146/annurev.cellbio.20.010403.095114

Reppert, S. M., & Wever, D. R. (2002). Coordination of circadian timing in mammals. *Nature*, *418*(August), 935–941. doi:10.1038/nature00965

Rink, J. C. (2013). Stem cell systems and regeneration in planaria. *Development Genes and Evolution*, *223*(1–2), 67–84. doi:10.1007/s00427-012-0426-4

Rouhana, L., Weiss, J. A., Forsthoefel, D. J., Lee, H., King, R. S., Inoue, T., … Newmark, P. A. (2014). RNA interference by feeding in vitro synthesized double-stranded RNA to

planarians : methodology and dynamics. *Developmental Dynamics*, *242*(6), 718–730. doi:10.1002/dvdy.23950.RNA

Sánchez Alvarado, A. (2006). Planarian regeneration: its end is its beginning. *Cell*, *124*(2), 241–245. doi:10.1016/j.cell.2006.01.012

Sanchez Alvarado, A., & Newmark, P. A. (1999). Double-stranded RNA specifically disrupts gene expression during planarian regeneration. *Proceedings of the National Academy of Sciences*, *96*(9), 5049–5054. doi:10.1073/pnas.96.9.5049

Schalbetter, S. A., Mansoubi, S., Chambers, A. L., Downs, J. A., & Baxter, J. (2015). Fork rotation and DNA precatenation are restricted during DNA replication to prevent chromosomal instability. *Proceedings of the National Academy of Sciences*, *112*(33), E4565–E4570. doi:10.1073/pnas.1505356112

Ünsal-Kaçmaz, K., Mullen, T. E., Kaufmann, W. K., & Sancar, A. (2005). Coupling of human circadian and cell cycles by the timeless protein coupling of human circadian and cell cycles by the timeless protein. *Current Biology*, *25*(8), 3109–3116. doi:10.1128/MCB.25.8.3109